American Mineralogist, Volume 84, pages 1577–1587, 1999

Hydrogen in diopside: Diffusion, kinetics of extraction-incorporation, and solubility

SARAH HERCULE AND JANNICK INGRIN*

Laboratoire des Mécanismes de Transferts en Géologie, CNRS UMR 5563, Equipe de Minéralogie, 39 Allées Jules Guesde, 31000 Toulouse, France

ABSTRACT

The kinetic of H extraction-incorporation in diopside single-crystals ($Ca_{0.97}Na_{0.02}Cr_{0.01}Mg_{0.97}Fe_{0.036}Si_{1.99}O_6$) deduced by monitoring OH infrared absorption bands for samples heated from 973 to 1273 K at 0.1 atm and 1 atm of pH_2, is independent of crystallographic orientation, P_{O_2}, and pH_2. The diffusion law is $D = D_0 \exp[-(126 \pm 24)$ kJ/mol/R$T]$, with log D_0 (in m^2/s) = -6.7 ± 1.1. Hydrogen self-diffusion obtained from H-D exchange in the same diopside samples over 873–1173 K, and along directions [001] and [100]* at 1 atm total pressure is two orders of magnitude faster than H uptake and follows the diffusion law $D_H = D_0 \exp[-(149 \pm 16)$ kJ/mol/R$T]$, with log D_0 (in m^2/s) = -3.4 ± 0.8. Self-diffusion along [010] follows the diffusion law $D_H = D_0 \exp[-(143 \pm 33)$ kJ/mol/R$T]$, with log D_0 (in m^2/s) = -5.0 ± 1.7 and is one order of magnitude faster than H uptake. The kinetics of extraction incorporation of H in this diopside follows the reaction $Fe^{3+} + O^{2-} + 1/2H_2$ (g) = $Fe^{2+} + OH^-$ and are not rate limited by the mobility of protons but more probably by the mobility of electron holes connected with the Fe oxidation-reduction process. The results suggest that the kinetics of H uptake in clinopyroxenes will increase with increasing Fe content until it is rate controlled by the kinetics of H self-diffusion. We predict a rate for H exchange in diopside appropriate to the upper mantle almost as fast as H exchange in olivine. The insensitivity of H solubility on temperature and P_{O_2} for samples recovered from low-temperature conditions (below 1273 K) and/or rapidly quenched samples let us suggest the use of OH concentration measurements in diopside as a potential pH_2 sensor.

INTRODUCTION

Water, stored as H defects, is commonly found in natural pyroxenes with concentrations ranging from 5 to 1100 ppm wt% H_2O (Skogby et al. 1990; Smyth et al. 1991; Bell and Rossman 1992). These values are large relative to the H contents of other upper mantle minerals like olivine or garnet. Consequently, Bell and Rossman (1992) argue that pyroxenes may be the main host phases for water in the upper mantle. However, the amount of water measured in xenoliths at the Earth's surface only indicates the amount preserved. Hydrogen exchange with magma might occur during the ascent of xenoliths. Mackwell and Kohlstedt (1990) measured a rate of H incorporation in olivine rapid enough to allow H outgassing during ascent from the upper mantle. They conclude that a low H content of olivine from mantle nodules is an insufficient proof of low H content of olivine in the upper mantle. Following the same line of reasoning, we have previously shown that the dehydrogenation rate in diopside is also rapid and leads to the same conclusion for clinopyroxene (Ingrin et al. 1995).

In contrast, Skogby and Rossman (1990) showed that H concentrations in pyroxenes correlate well with geological environment; a signature of hydrous activity is thus preserved in these minerals. A better understanding of the mechanisms and kinetics of dehydrogenation-hydrogenation in diopside is necessary to constrain better the conditions of this preservation.

Several authors proposed H to be mainly accommodated in Fe-bearing crystals by charge compensation through the following reaction (Clowe et al. 1988; Dyar et al. 1993 for amphiboles; Mackwell and Kohlstedt 1990 for olivine; Ingrin et al. 1989; Skogby and Rossman 1989; Skogby 1994 for diopside):

$$Fe^{3+} + O^{2-} + 1/2H_2\,(g) = Fe^{2+} + OH^- . \quad (1)$$

It is generally assumed that the kinetics of this reaction are rate limited by H diffusion but this has yet to be demonstrated clearly.

To clarify these issues, we have performed incorporation experiments by annealing diopside in H, at partial pressures of 0.1 and 1 atm, and performed deuteration experiments in the same samples to measure H self diffusivities by kinetic studies of isotope exchange.

*E-mail: ingrin@cict.fr

EXPERIMENTAL TECHNIQUES

Starting material

The samples are thin slices of a Russian diopside single crystal with X_{Fe} = 0.036 [X_{Fe} = Fe/(Fe + Mg) cation ratio] as described and enumerated by Ingrin et al. (1995). Some samples were repolished, reducing thickness by a few micrometers. Cuts are parallel to the (100) and (010) crystallographic planes and perpendicular to the [001] axis (labeled directions [100]*, [010], and [001], respectively) (Table 1).

TABLE 1. Experimental data for hydrogen uptake

Sample	Orientation	P_{O_2} (atm)	pH_2 (atm)	t (h)	$t$cor. (h)	A (cm^{-1})	ΔA (cm^{-1})
		1273 K; 2 L = 0.932 mm; size: 4.6 ↔ 4.1 mm²					
IV	[001]	10^{-16}	0.1	5.00	5.47	1.18	0.2
				15.00	15.95	2.68	0.3
				25.00	26.39	3.39	0.3
				35.00	36.85	3.34	0.3
				55.00	57.31	4.77	0.4
				75.00	77.77	4.23	0.3
				89.00	92.23	4.48	0.3
				95.00	98.69	4.50	0.3
				105.00	109.15	4.50	0.3
		1273 K; 2 L = 0.945 mm; size: 6.0 ↔ 3.0 mm²					
VI	[100]*	10^{-16}	0.1	5.00	5.47	2.53	0.2
				10.00	10.94	3.33	0.4
				20.00	21.41	3.92	0.5
				40.00	41.88	4.28	0.5
				60.00	62.35	5.10	0.4
				80.00	82.82	5.02	0.4
				120.00	123.29	5.02	0.7
		1173 K; 2 L = 0.548 mm; size: 8.5 ↔ 3.8 mm²					
III	[001]	$4\ 10^{-18}$	0.1	10.00	10.48	1.47	0.5
				20.00	20.96	2.05	0.3
				30.00	31.44	2.03	0.3
				40.00	41.92	2.96	0.2
				50.00	52.40	2.96	0.3
		1173 K; 2 L = 0.533 mm; size: 8.5 ↔ 3.8 mm²					
III	[001]		1	5.00	5.53	2.68	0.3
				10.00	11.06	3.58	0.3
				15.00	16.59	4.51	0.4
				20.00	22.12	5.15	0.4
				40.00	42.56	6.31	0.3
				60.00	63.18	6.58	0.3
				123.25	126.96	6.76	0.2
		1079 K; 2 L = 0.973 mm; size: 4.3 ↔ 4.1 mm²					
I	[001]	$3\ 10^{-20}$	0.1	50.00	51.35	1.54	0.4
				90.00	91.80	2.78	0.4
				130.00	132.25	3.61	0.3
				190.00	192.70	4.82	0.3
				250.00	253.15	5.09	0.3
				330.00	333.60	5.15	0.3
		983 K; 2 L = 0.606 mm; size: 4.0 ↔ 5.0 mm²					
IX	[100]*		1	30.00	30.58	8.34	0.5
				60.00	61.16	10.79	0.5
				94.00	95.74	11.45	0.5
				135.92	138.24	12.47	0.7
				190.00	192.90	13.21	0.6
				243.89	247.37	13.87	0.5
				309.14	313.20	14.25	0.6
				373.47	378.11	14.71	0.6
				442.42	447.64	14.99	0.4
				561.42	567.22	15.18	0.5

Note: t is the nominal time of heating, *t*cor. the time of heating after correction due to the durations of the heating ramps, A = the OH integral absorbance, ΔA = the uncertainty on A, and 2 L = the thickness of the sample.

Annealing procedures

Heat treatments for both H incorporation and deuteration experiments were carried out in a horizontal furnace. An alumina tube 18 mm in internal diameter and a silica glass tube of 60 mm in internal diameter were used for the experiments at 0.1 atm pH_2 and 1 atm pH_2, respectively. Temperatures ranged from 873 to 1273 K, and were controlled by a Pt/Pt-Rh10% thermocouple located less than 5 mm from the sample. We estimate the uncertainty in temperature to be less than ±5 °C mainly due to furnace gradients and variations in room temperature.

The reducing atmosphere around the samples was fixed by either a gas mixture of 90%Ar + 10%H_2 flowing through water (pH_2 = 0.1 atm) and pure H at 1 atm (pH_2 = 1 atm) for H uptake, or 90%Ar + 10%D_2 flowing through deuterated water (99.8% D_2O; pD_2 = 0.1 atm) and 90%Ar + 10%H_2 flowing through water for H-D and D-H exchange experiments. The oxygen partial pressure, through water dissociation equilibrium, ranged from 10^{-25} to 10^{-16} atm, depending on the temperature for experiments performed with pH_2 or pD_2 equal to 0.1 atm (Tables 1 and 2). We checked the values of P_{O_2} with a zirconia sensor (with internal solid Pd/PdO reference) placed in an independent furnace working at 1073 K and connected to the outlet of the experimental device. The measured values fall within one order of magnitude of those calculated from gas proportions. The exact P_{O_2} of the experiments performed at 1 atm pH_2 is unknown.

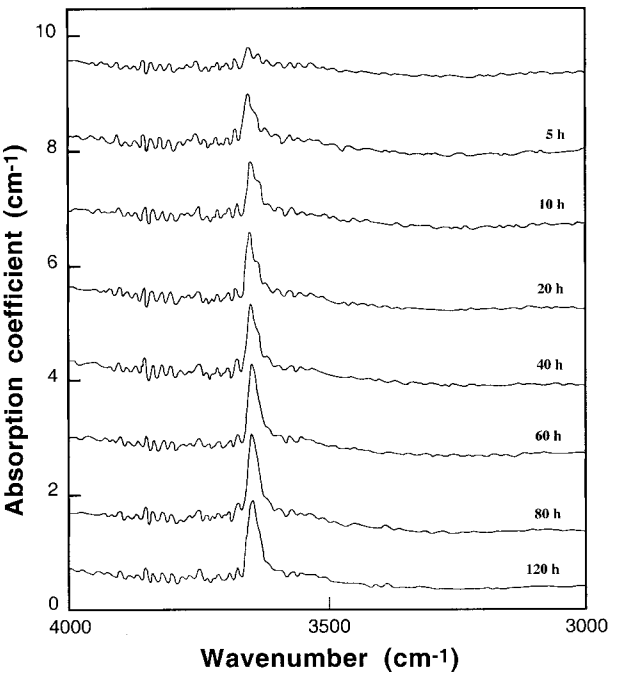

FIGURE 1. Evolution of IR absorption spectra with increasing time of heating. Sample VI, cut perpendicular to the [100]* direction was annealed at 1273 K in a pH_2 of 0.1 atm for up to 120 hours. Spectra were taken with a circular aperture of 1.5 mm in diameter at a resolution of 2 cm^{-1} and smoothed afterward.

TABLE 2. Experimental data for H→D and D→H exchange

Exchange H→D				Exchange D→H		
t (h)	t cor. (h)	A_D (cm^{-1})	ΔA_D (cm^{-1})	t cor. (h)	A_D (cm^{-1})	ΔA_D (cm^{-1})
XI [010] 1173 K and 2 L = 0.746 mm						
0.00	0.00	–	–	0.00	1.24	0.08
0.20	0.60	0.43	0.06	0.67	0.88	0.05
0.40	1.20	0.63	0.06	1.34	0.60	0.08
0.80	2.00	0.88	0.06	2.21	0.31	0.06
1.60	3.20	1.04	0.07	3.48	0.17	0.06
11.60	13.60	1.22	0.08	13.95	–	–
23.60	26.00	1.24	0.08			
VI [100]* 1133 K, 1139K and 2 L = 0.945 mm						
0.00	0.00	–	–	0.00	2.78	0.10
0.17				1.36	0.78	0.10
0.33				2.72	0.30	0.06
0.50	0.92	2.43	0.08			
1.00	1.84	2.78	0.10			
VI [100]* 1073 K and 2 L = 0.945 mm						
0.00	0.00	–	–	0.00	2.78	0.10
1.00	1.31	2.05	0.06	1.36	0.78	0.10
2.00	2.62	2.50	0.09	2.72	0.30	0.06
3.00	3.93	2.63	0.08			
5.00	6.24	2.66	0.10			
7.00	8.55	2.78	0.10			
22.00	23.86	2.78	0.10			
I [001] 1073 K and 2 L = 0.973 mm						
0.00	0.00	–	–	0.00	2.21	0.05
0.50				0.86	0.83	0.04
1.00	1.31	1.88	0.05	1.72	0.38	0.07
2.00	2.62	2.08	0.04			
8.00	8.93	2.16	0.04			
16.00	17.24	2.21	0.05			
XI [010] 1073 K and 2 L = 0.746 mm						
0.00	0.00	–	–	0.00	1.17	0.10
1.00				1.36	0.87	0.07
2.00	2.30	0.55		2.72	0.63	0.10
4.00	4.60	0.70	0.04	5.02	0.50	0.10
8.00				9.44	0.25	0.10
20.00	20.80	1.18	0.10			
40.00	41.12	1.17	0.10			
VI [100]* 973 K and 2 L = 0.945 mm						
0.00	0.00	–	–	0.00	2.72	0.10
1.00	1.28	0.94	0.07	1.34	1.74	0.09
2.00	2.56	1.44	0.05	2.38	1.30	0.07
3.00	3.84	1.87	0.04			
4.00	5.12	2.07	0.10	5.02	0.86	0.13
8.00	9.40	2.44	0.10	9.36	0.45	0.20
16.00	17.68	2.72	0.10			
35.00	36.96	2.71	0.10			
I [001] 973 K and 2 L = 0.973 mm						
0.00	0.00	–	–	0.00	2.36	0.10
1.00	1.28	0.92	0.04	1.34	1.40	0.06
2.00	2.56	1.36	0.03	2.68	1.13	0.04
3.00	3.84	1.49	0.04	4.02	0.81	0.06
4.00				5.36	0.63	0.07
6.00	7.12	1.88	0.06	7.70	0.44	0.06
20.00	21.4	2.33	0.10			
40.00	41.68	2.36	0.10			
XI [010] 973 K and 2 L = 0.746 mm						
0.00	0.00	–	–			
4.00	4.84	0.22	0.09			
8.00	9.12	0.33	0.05			
14.00	15.40	0.51	0.04			
28.00	28.68	0.79	0.10			
48.00	49.96	1.05	0.10			
78.00	80.24	1.25	0.07			

TABLE 2.—*Continued*

Exchange H→D				Exchange D→H		
t (h)	t cor. (h)	A_D (cm^{-1})	ΔA_D (cm^{-1})	t cor. (h)	A_D (cm^{-1})	ΔA_D (cm^{-1})
VI [100]* 873 K and 2 L = 0.945 mm						
0.00	0.00	–	–	0.00	2.70	0.00
1.00				1.34	2.41	0.04
2.00	2.28	0.28	0.10	2.68	2.35	0.05
4.00	4.56	0.45	0.10	5.02	2.11	0.02
8.00	8.84	0.66	0.15	9.36	1.93	0.07
20.00	21.12	1.23	0.09	21.70	1.53	0.08
40.00	41.40	1.79	0.09	42.04	1.13	0.10
60.00	61.68	2.09	0.12			
80.00	81.96	2.34	0.13	82.38	0.55	0.10
130.00	132.24	2.61	0.06			
180.00	182.52	2.70	0.07			
I [001] 873 K and 2 L = 0.973 mm						
0.00	0.00	–	–			
1.00						
2.00	2.28	0.59	0.04			
4.00	4.56	0.69	0.04			
8.00	8.84	0.93	0.06			
20.00	21.12	1.18	0.06			
40.00	41.40	1.69	0.04			
60.00	61.68	1.91	0.03			
80.00	81.96	1.99	0.02			
120.00	122.24	2.18	0.05			
200.00	202.52	2.25	0.10			

Note: t is the nominal time of heating, t cor. the time of heating after correction due to the durations of the heating ramps, A = the OH integral absorbance, ΔA = the uncertainty on A, and 2 L = the thickness of the sample.

The samples were held vertically on MgO plates to avoid any chemical reactions between alumina and diopside. The tube was flushed with the gas mixture for 30 min before heating started. A ramp was programmed to reach the final temperature within 60 to 100 minutes.

Before any incorporation experiments, we annealed the samples in air to remove completely the H present inside the crystal. For samples cut parallel to (100), we observed slight residual absorption bands at 3645 cm^{-1} and 3530 cm^{-1} (Fig. 1), which we took into account in our analytical treatment.

Infrared analysis

Infrared absorption spectra were obtained at room temperature by accumulating 64 scans with a resolution of 2 cm^{-1}, without a polarizer (FTIR Spectrometer Perkin Elmer 1600, which was purged in N_2). Each spectrum was collected on the central part of the sample through an aluminum foil aperture of 1.5 or 2 mm in diameter, and then smoothed to a resolution of 22 cm^{-1}. We measured the integral of the absorbance, A, by subtracting a linear baseline estimated visually, in the range of wavenumbers 3725–3440 cm^{-1} and 3725–3256 cm^{-1} for [001] and [100]* directions, respectively. Errors on measurements of absorbance were estimated from the reproducibility of the spectral analysis and the fluctuations in A due to variations in the estimation of the baseline (see Ingrin et al. 1995).

Analytical solution

Because the thickness of the sample is small compared to its width, we assume that diffusion is essentially one dimensional and can be described by equations for a solid bounded

by two parallel planes. The general solution of Fick's second law, for an average H concentration, C_{avg}, integrated over the whole thickness (Carslaw and Jaeger 1959) in the case of H uptake is:

$$\frac{C_{av}(t)}{C_S} = 1 + \frac{8(C_0 - C_s)}{\pi^2 C_s} \sum_{n=0}^{\infty} \frac{1}{(2n+1)^2} \exp\left(\frac{-D\,(2n+1)^2 \pi^2 t}{4L^2}\right). \quad (2)$$

with the following boundary conditions: at $t = t_0$, for $-L < x < +L$, $C(x) = C_0$, the initial concentration, and at any t, for $x = -L$ and $x = +L$, $C(x) = C_s$, the H concentration at saturation; where t_0 is the initial time, L is the half thickness of the sample and D is the diffusion coefficient of the mobile species. In most cases, H was completely removed from the sample before the experiment ($C_0 = 0$) and we used the following solution:

$$\frac{C_{av}(t)}{C_S} = 1 - \frac{8}{\pi^2} \sum_{n=0}^{\infty} \frac{1}{(2n+1)^2} \exp\left(\frac{-D\,(2n+1)^2 \pi^2 t}{4L^2}\right). \quad (3)$$

In H-D exchange experiments, we followed the integral of absorbance of the O-D bands that are located in a less noisy wavenumber range of the spectrum. Expression 3 is also valid for the analysis of the D → H exchange experiments (D replaced by H), while for the reverse boundary conditions (H → D experiments, H replaced by D), C_{avg}/C_0 is equal to (1 – Equation 3).

For experiments of H-D exchange performed in sample XI along direction [010], a three-dimensional diffusion fitting function was used to take account of possible lateral diffusion from other directions due to the lower diffusion rate along [010]. Data were fit to Equation 4, which is a function of the sample dimensions x, y, and z (0.746, 3.3, and 4.4 mm, respectively), the diffusion coefficients D_y and D_z along [001] and [100]* directions (deduced from experimental measurements) and the size of the IR aperture [assuming a square aperture of side $2d$; here $2d$ = 1.329 mm; see Ingrin et al. (1995) for more details]:

$$\frac{C_{avg}(t)}{C_S} = 1 - \frac{512xy}{\pi^6 d^2} \sum_{l=0}^{\infty} \sum_{m=0}^{\infty} \sum_{n=0}^{\infty} \frac{(-1)^{m+n}}{(2l+1)^2 (2m+1)^2 (2n+1)^2} \exp\left(\frac{-D_x\,(2l+1)^2 \pi^2 t}{4L^2}\right) \exp\left(\frac{-D_y\,(2m+1)^2 \pi^2 t}{4y^2}\right) \exp\left(\frac{-D_z\,(2n+1)^2 \pi^2 t}{4z^2}\right) \sin\frac{(2m+1)\pi d}{2y} \sin\frac{(2n+1)\pi d}{2z} \quad (4)$$

We apply the same correction to time, t_{cor} as described by Ingrin et al. (1995), to take account of the time to reach the final "plateau" temperature and to quench the samples.

RESULTS

Hydrogen incorporation

OH IR bands are restored after annealing dried samples in H at 1 atm pressure, with a peak height depending on H partial pressure. The IR spectra are dominated by the band at 3645 cm^{-1} and, for samples oriented along [100]*, spectra exhibit a second weaker band around 3530 cm^{-1} (Fig. 1; incorporation at 1273 K and 0.1 atm pH_2), similar to that observed in the untreated samples, but with a lower intensity (see Fig. 2 in Ingrin et al. 1995).

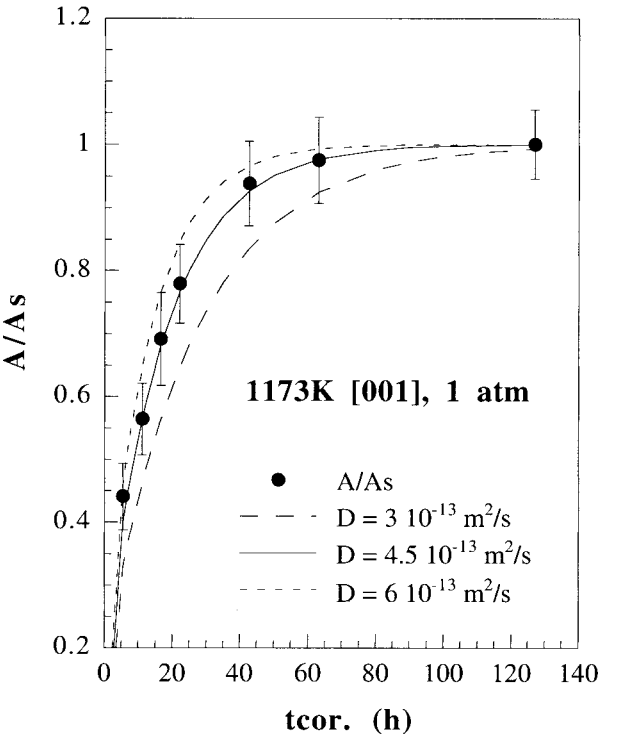

FIGURE 2. Fit of hydrogen incorporation data by Equation 2 for different values of D. Sample III, 1173 K, [001], 1 atm pH_2. Error bars on D were deduced from the range of D values that still fit the data (dashed lines).

We measured the uptake of H as a function of time through the evolution of the OH integral absorbance, A, with the cumulative time of heating (Table 1). We assume the ratio $C_{avg}(t)/C_s$ to be equivalent to $A(t)/A_s$, following Beer's law (A_s is the value of the integral absorbance at saturation). Thickness of samples is constant during the succession of runs. The fit of the values of absorbance by Equations 2 and 3 leads to the determination of the diffusion coefficient D (see Fig. 2 for an example of fits), assuming that D is independent of the H concentration within the crystal. The error bars on D are estimated by the extreme values that still fit the data within the experimental uncertainty on A (Fig. 2).

The present results for H incorporation are close to the D values found for the kinetics of H extraction from Ingrin et al. (1995) (Fig. 3) and can be considered identical within the error of the measurements. Thus, the results confirm the reversibility of the kinetics of the reaction controlling the extraction-incorporation of H in diopside in the temperature range 973–1273 K. The kinetics of extraction-incorporation is not dependent on H partial pressure as indicated by annealing at 1173 K but

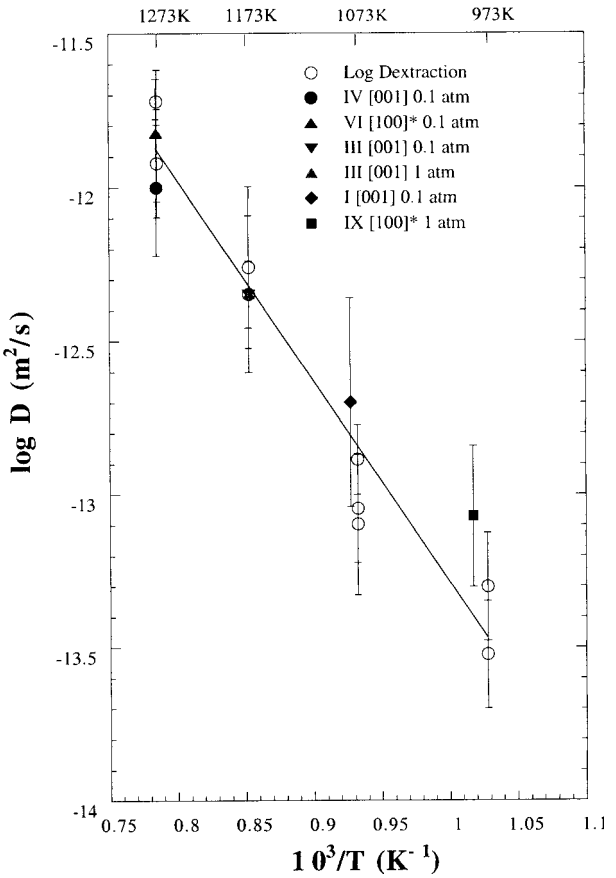

FIGURE 3. Arrhenius diagram showing the comparison between H incorporation data along [100]* and [001] directions (filled symbols) and H extraction data from Ingrin et al. (1995) (open symbols). The solid line represent a least squares fit to all of the data.

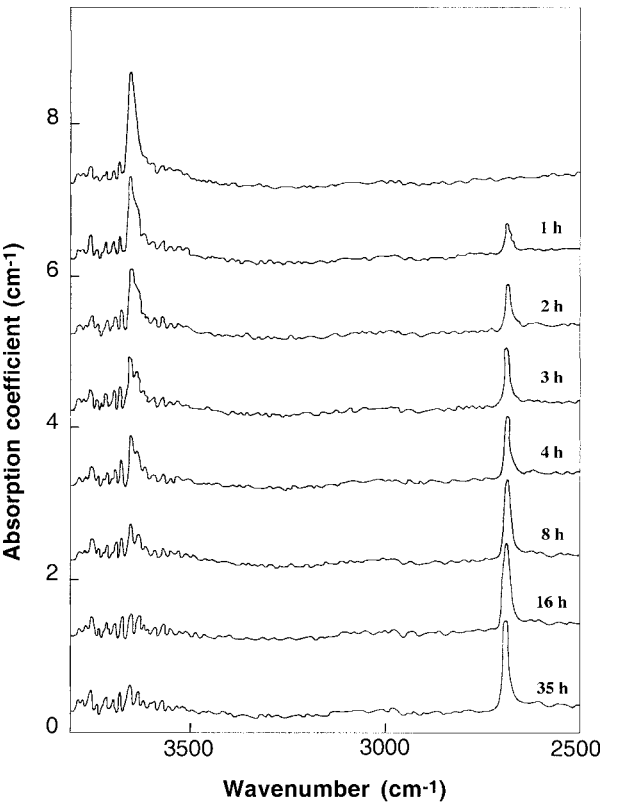

FIGURE 4. IR absorption spectra, showing the progressive replacement of OH absorption bands by OD absorption bands, with successive time of heating. Sample VI was heated at 973 K and a pD_2 of 0.1 atmosphere. Spectra were taken with a circular aperture 1.5 mm in diameter at an initial resolution of 2 cm^{-1} and smoothed afterward.

different pH_2 (0.1 and 1 atm), and extraction performed in air (Ingrin et al. 1995). No dependence is also observed on P_{O_2} in the range 10^{-16} to 10^{-25} atm or extraction performed in air (P_{O_2} = 0.21 atm, Ingrin et al. 1995). Experiments at 1273 K performed in both directions [001] and [100]* confirm that the kinetics of H incorporation is the same for both directions. No kinetic study of incorporation was performed for the [010] direction. However the similarity of the results with those from extraction experiments, where the [010] direction was tested, confirms (as noted in Ingrin et al. 1995) that H extraction-incorporation in this diopside is isotropic.

A least-squares fit to all data (extraction and incorporation data), using the York's method (1966) leads to the following Arrhenius law:

$$D = D_0 \exp\left(\frac{-(126 \pm 24)\text{kJ / mol}}{RT}\right) \text{ with } \log D_0 \text{ (in m}^2\text{/s)} = -6.7 \pm 1.1. \quad (5)$$

The uncertainties on the activation enthalpy and $\log(D_0)$ are equal to 3**s** with σ the standard deviation deduced from the linear least squares regression.

H-D exchange

After H saturation of diopside slices at pH_2 of 0.1 atm, we annealed them in the deuterated gas mixture, at a pD_2 of 0.1 atm. OH absorption bands are progressively replaced by OD bands (Fig. 4). Absorbance due to the OD band occurs at 2689 cm^{-1}. The observed spectral wavenumber shift (n_{OH}/n_{OD}) is equal to 1.35, near to the expected 1.36 value deduced from the reduced masses of O-D and O-H stretching dipoles. For samples oriented along [100]*, a shoulder at 2618 cm^{-1} is observed, which presumably corresponds to the shift of the 3530 cm^{-1} band (Fig. 4).

Figure 5 shows the evolution of the concentration of H, C_H vs. that of deuterium C_D normalized to the concentration at saturation for a sample cut perpendicular to directions [001] and annealed at 973 K ($C_H = A_H/A_{Hs}$; $C_D = A_D/A_{Ds}$; A_H, A_D, and A_{Hs}, A_{Ds} are the integral absorbance of OH and OD bands and their value at saturation, respectively). The constant slope of near –1 confirms that there is a 1:1 exchange and no decrease of H + D concentration within the sample. The value of the integral absorbance due to the band related to deuterium at saturation A_{Ds}, compared to that of H, A_{Hs}, allowed us to estimate the ratio of the

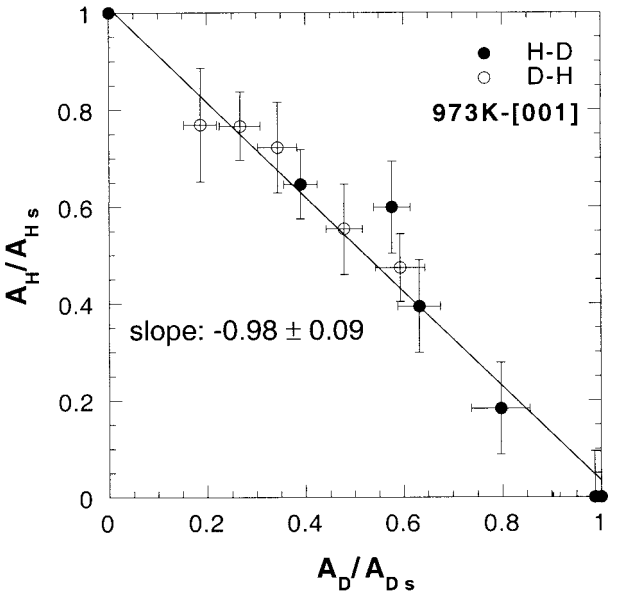

FIGURE 5. Normalized OH integral absorbance, A_H/A_{Hs}, vs. normalized OD integral absorbance, A_D/A_{Ds}, during successive annealings at 973 K (sample I).

molar absorptivity of OH vs. OD, $\varepsilon_H/\varepsilon_D$, according to Beer's law

$$\left(\frac{A_H}{A_D} = \frac{\varepsilon_H \times \text{path length} \times C_{OH}}{\varepsilon_D \times \text{path length} \times C_{OD}} = \frac{\varepsilon_H}{\varepsilon_D}\right).$$

The value of $\varepsilon_H/\varepsilon_D$ seems to be higher for measurements along direction [010] (1.7 ± 0.3 and 1.8 ± 0.3 are the average values for samples [100]* and [001] vs. 2.2 ± 0.4 for the direction [010]). As these values are very similar we calculated an average value of $\varepsilon_H/\varepsilon_D$ from all experiments of 1.9 ± 0.3.

The integral absorbance of OD is presented in Table 2, when deuterium replaces H in the sample (H → D exchange) and for the reverse case (D → H exchange). In the same manner as for the determination of the kinetics of H uptake, we fit the data for directions [001] and [100]* using Equation 3 to determine the deuterium diffusion coefficient. The rates of H → D and D → H exchange are very similar (solid circles for AD/ADs in H→D experiments; empty circles for reversed D → H experiments, Fig. 6). The experiments performed in both [001] and [100]* directions exhibit essentially the same diffusion coefficients. The diffusion along the [010] direction is about one order of magnitude slower than for the two other directions. Thus, for this direction, a fit by the three-dimensional diffusion law (Eq. 4) is required (see examples of fits in Fig. 6). Diffusion data are listed in Table 3 and the plot of those data on an Arrhenius diagram leads to the following diffusion laws:

$$D = D_0 \exp\left(\frac{-(149 \pm 16)\text{kJ/mol}}{RT}\right), \text{ for [100]* and [001] with } \log D_0 \text{ (in m}^2\text{/s)} = -3.4 \pm 0.8. \quad (6)$$

$$D = D_0 \exp\left(\frac{-(143 \pm 33)\text{kJ/mol}}{RT}\right), \text{ for [010] with } \log D_0 = -5.0 \pm 1.7. \quad (7)$$

As for the treatment of the incorporation data, uncertainties on the activation energy and $\log D_0$ are the 3σ values determined from the fitting procedure. With a mass two times higher than that of H, D should be the slower species in the H-D exchange. However, the correction due to the mass effect is generally assumed to be of the order of 1.4 $[(m_D/m_H)^{1/2}$; Le Claire 1966], below the average experimental uncertainty of the diffusion measurements. Thus, we will assume in the following that the above diffusion laws represent the self-diffusion of H or D in diopside.

The kinetics of H-D exchange is very rapid, compared to the kinetics of H extraction-incorporation measured in the same samples (at least two orders of magnitude faster for directions [100]* and [001]; Fig. 7).

Solubility

Incorporation experiments give the opportunity to study the dependence of H solubility in diopside on temperature and pH_2. Table 4 shows the results of integral absorption measurements after successive annealing up to saturation, from 973 to 1273 K. We checked that saturation in the sense of Equation 1 is reached, at each temperature, when the integral absorbance is no longer varying with time of heating. The absorbances (A_s) normalized to 1 cm thickness (Table 4) show that there is no effect of temperature on H solubility at a pH_2 of 1 atm in the range of temperatures 973–1273 K (see samples I, V, VI, Table 4). However, for the same gas mixture (in this case, 90%Ar-10%H_2 flowing through water), and for a constant pH_2, P_{O_2} is a function of

TABLE 3. Diffusion coefficients for H-D exchange and hydrogen uptake

Sample	Orientation	T (K)	Exchange m^2/s	$D_{H\text{-}D}$	D_{uptake} m^2/s
VI	[100]*	1273			$(1.5 \pm 0.5)\ 10^{-12}$
IV	[001]	1273			$(1.0 \pm 0.4)\ 10^{-12}$
III	[001]	1173			$(5 \pm 2)\ 10^{-13}$
XI	[010]	1173	H-D	$(3 \pm 1.8)\ 10^{-12}$	
VI	[100]*	1133	H→D	$(5 \pm 1)\ 10^{-11}$	
VI	[100]*	1139	D→H	$(4 \pm 1)\ 10^{-11}$	
VI	[100]*	1073	H→D	$(2 \pm 1)\ 10^{-11}$	
VI	[100]*	1073	D→H	$(2 \pm 0.5)\ 10^{-11}$	
I	[001]	1073	H→D	$(3 \pm 1)\ 10^{-11}$	$(2 \pm 3)\ 10^{-13}$
I	[001]	1073	D→H	$(2.5 \pm 0.5)\ 10^{-11}$	
XI	[010]	1073	H-D	$(1.4 \pm 0.5)\ 10^{-12}$	
IX	[100]*	983			$(8.5 \pm 2.5)\ 10^{-14}$
VI	[100]*	973	H→D	$(6 \pm 1)\ 10^{-12}$	
VI	[100]*	973	D→H	$(5 \pm 1)\ 10^{-12}$	
I	[001]	973	H→D	$(6 \pm 1)\ 10^{-12}$	
I	[001]	973	D→H	$(6 \pm 1)\ 10^{-12}$	
XI	[010]	973	H→D	$(1.8 \pm 0.8)\ 10^{-13}$	
VI	[100]*	873	H→D	$(5 \pm 1)\ 10^{-13}$	
VI	[100]*	873	D→H	$(4 \pm 1)\ 10^{-13}$	
I	[001]	873	H→D	$(8 \pm 1)\ 10^{-13}$	

Note: H→D correspond to exchange of hydrogen by deuterium and D→H for the opposite exchange deducted from fitting of a one dimension law. H-D corresponds to fits realized considering both exchanges. For sample XI (orientation [010]), a three dimensional fit was used.
* D_{uptake} are the diffusion coefficients obtained for hydrogen uptake.

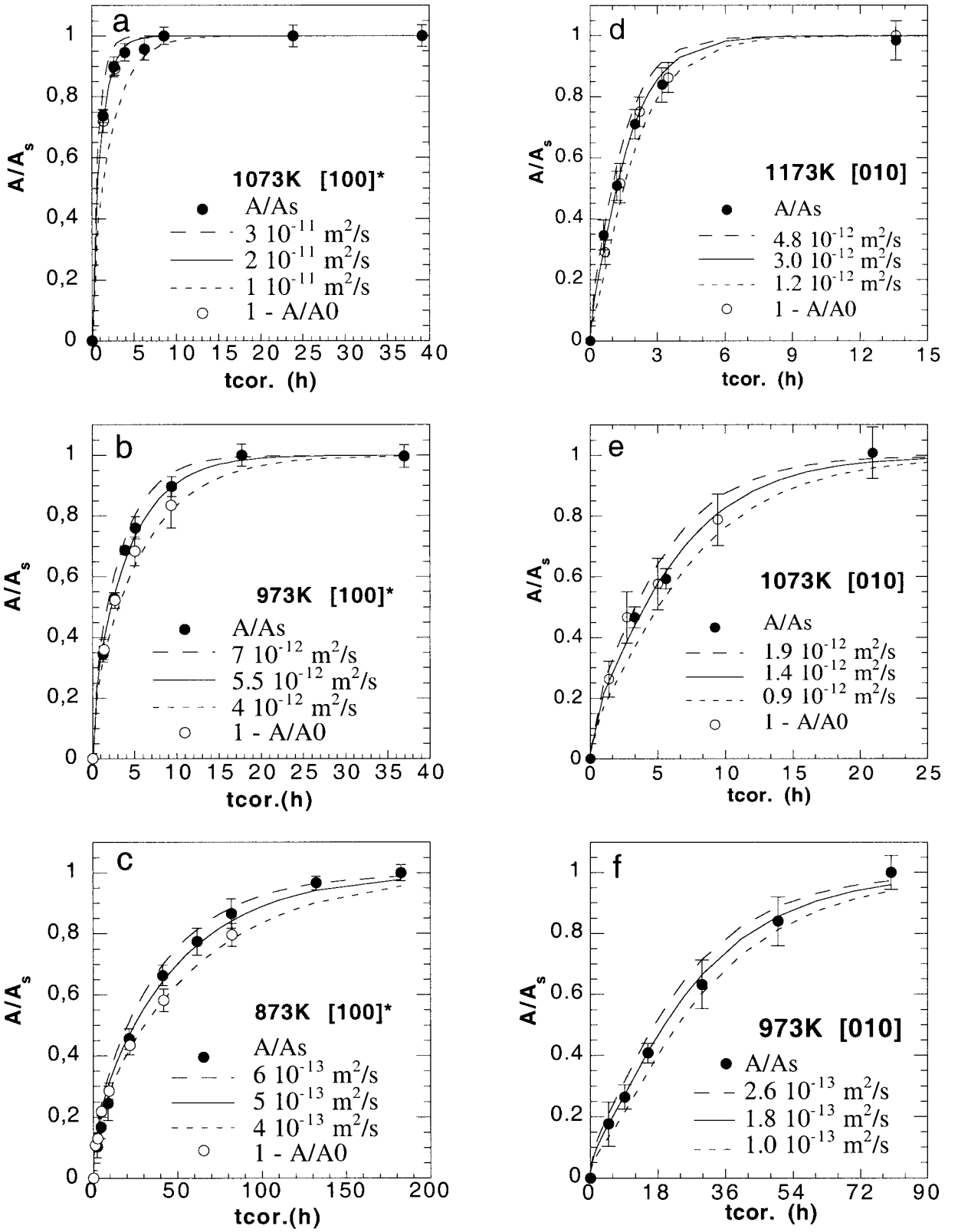

FIGURE 6. Fit of deuteration data by Equation 3 with different values of D, for sample VI cut perpendicular to [100]* (a, b, c), and Equation 4 for sample XI cut perpendicular to [010] (d, e, f). Solid circles represent the results of H → D exchange (D entering into the crystal) and empty circles the results of D → H exchange (H entering into the crystal).

TABLE 4. OH integral absorption at saturation

Sample	P_{O_2} (atm)	T (K)	pH_2 (atm)	A_s (cm^{-2})	ΔA_s (cm^{-2})
IV [001]	10^{-16}	1273	0.1	48.3	3.2
IV [001]	10^{-18}	1273	0.1	49.4	3.3
IV [001]	?	1273	1.0	107.3	5.4
III [001]	$4\ 10^{-18}$	1173	0.1	54.0	5.5
III [001]	?	1173	1.0	115.6	3.7
I [001]	$3\ 10^{-20}$	1079	0.1	52.9	3.1
I [001]	?	1073	1.0	99.5	4.1
I [001]	10^{-25}	873	0.1	52.0	4.2
I [001]	10^{-22}	973	0.1	53.8	4.2
I [001]	$3\ 10^{-20}$	1073	0.1	55.5	4.2
I [001]	10^{-16}	1273	0.1	51.3	4.2
V [001]	10^{-22}	973	0.1	75.8	10.0
V [001]	?	973	1.0	149.0	17.0
V [001]	?	973	1.0	149.5	7.5
V [001]	?	1073	1.0	140.7	7.5
V [001]	?	1173	1.0	145.2	7.5
V [001]	?	1273	1.0	149.0	10.0
VI [100]*	10^{-25}	873	0.1	53.8	4.1
VI [100]*	10^{-22}	973	0.1	55.5	3.1
VI [100]*	$3\ 10^{-20}$	1073	0.1	51.3	4.1
VI [100]*	10^{-16}	1273	0.1	53.1	7.4

Note: T is the annealing temperature, pH_2 the hydrogen partial pressure, A_s the integral absorption of the OH bands at saturation normalized to 1 cm thickness and ΔA_s the uncertainty on A_s.

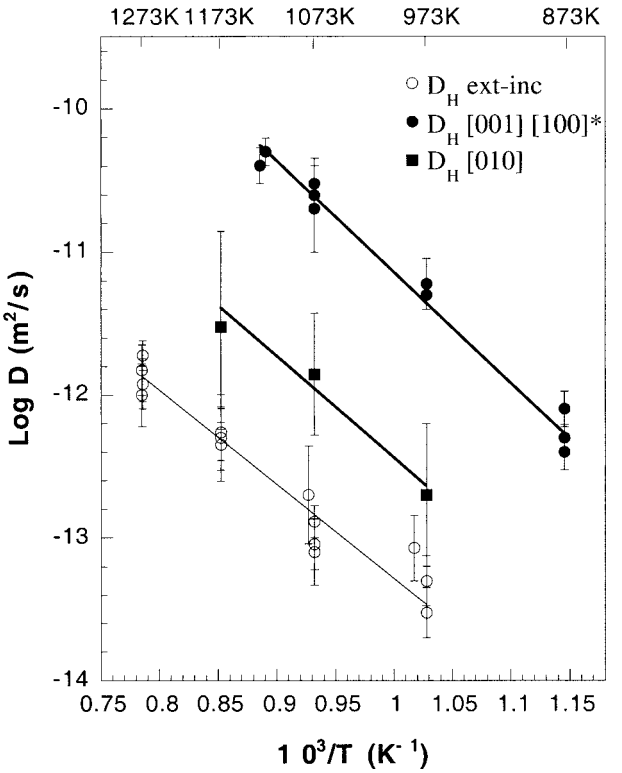

FIGURE 7. Summary of Arrhenius plots showing diffusion coefficients of hydrogen $D_{H[001]\ [100]^*}$ and $D_{H[010]}$ deduced from deuteration data compared to diffusion coefficients calculated for the extraction-incorporation process of H in diopside.

temperature (Table 4). To check if the observed independence of the solubility on temperature is unaffected by a correlated change of P_{O_2}, we performed an experiment at 1273 K on a same sample (sample IV, Table 4) at 0.1 atm pH_2 with two different gas mixtures (90%Ar-10%H_2 flowing into water and direct 90%Ar-10%H_2 without water) leading respectively to two different values of P_{O_2}: 10^{-18} and 10^{-16} atm (measured by the P_{O_2} cell). No variation of the solubility was observed for this 2 orders of magnitude variation of the P_{O_2}. Considering the uncertainty of IR measurement this observation suggests that no dependence of solubility on P_{O_2} occurs in this range of P_{O_2} or the dependence is very weak, if described by a power law ($C_s \propto P_{O_2}^m$) corresponds to a value of m lower than 1/20.

The integral absorbance A_s at saturation of slices cut along (001) from 973 to 1273 K, at both 0.1 and 1 atm pH_2 may change up to a factor 2 from one slice to another (Table 4), but the ratio of absorbance at a pH_2 of 1 atm over absorbance for a pH_2 of 0.1 atm is quite constant and show no strong dependence on temperature (Fig. 8). The data (Table 4) can be fit to a power law relation:

$$C_s \propto A_s \propto (pH_2)^m, \quad (8)$$

where m is the H partial pressure exponent. The average value of the solubility ratio for different samples yields m = 0.31 ± 0.03 (Fig. 8).

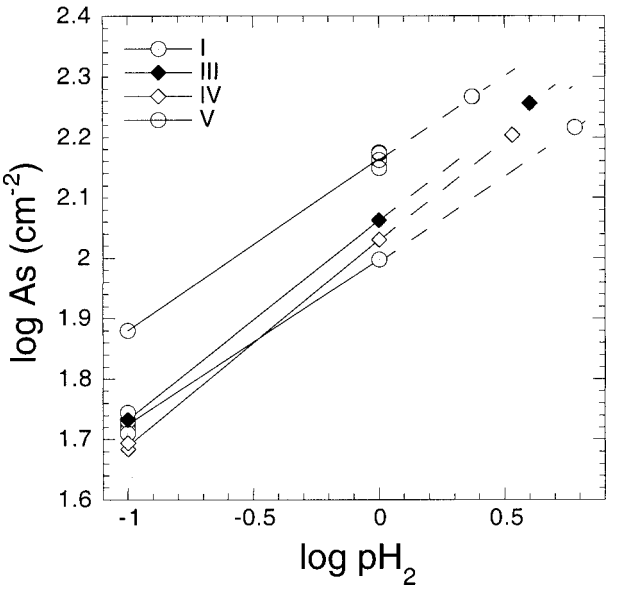

FIGURE 8. Logarithm of the OH integral absorption at saturation, As for samples I, III, IV, V, oriented along [001], as a function of log (pH_2). Symbols in the shaded area correspond to integral absorption values measured in as-grown crystals (Ingrin et al. 1995). The range of pH_2 predicted for these samples during formation is 2 to 6 atm.

DISCUSSION

The kinetics data from incorporation experiments confirm the analysis of data collected on the same samples from H extraction experiments (Ingrin et al. 1995), whereas H-D exchange performed also on the same samples show faster kinetics for H

mobility in diopside. These results imply a revision of the previous interpretations of the rate limiting mechanism operating in H incorporation-extraction in diopside (Ingrin et al. 1995). Incorporation experiments performed at low temperature (below 1273 K) give some constraints on the evolution of H solubility with imposed external pH_2. Few equilibration experiments performed in a natural sample at different pH_2 is enough to calibrate this sample as an independent pH_2 sensor.

Kinetics of hydrogen incorporation

As in Ingrin et al. (1995), we have only investigated the relative change of H concentration with time of heating and we assume that Beer's law is valid for diopside over the range used for the integration of the absorbance spectra (3725 to 3256 cm^{-1}). We observed no significant difference in the rate of increase (or decrease) of OH bands at 3645 and 3355 cm^{-1}. The size and thickness of the samples are almost the same as the original samples used in Ingrin et al. (1995); thus, as shown in this previous paper, the assumption of one-dimensional diffusion is valid as long as diffusion is isotropic. The kinetics of the H extraction-incorporation process in diopside in the temperature range 973–1273 K is thus reversible, isotropic, and independent of P_{O_2} and pH_2.

Hydrogen diffusion in diopside

The diffusion coefficients obtained from H-D exchange experiments (Eqs. 6 and 7) are assumed to represent the H self-diffusion coefficient in diopside. From the compilation of diffusion data (Fig. 9), H has the fastest diffusion coefficient of any species measured in diopside. Diffusion of Ca and Sr in diopside show isotropic behavior at least within the experimental uncertainties of measurements (Sneeringer et al. 1984; Dimanov et al. 1995). The anisotropy of Si and Al diffusion has not been tested, but oxygen diffusion data collected on natural samples by Farver (1989) through hydrothermal experimental conditions show that diffusion perpendicular to the [001] direction of diopside is fifty times slower than diffusion along the [001] direction (Fig. 9). Unfortunately, the exact direction of diffusion perpendicular to [001] is not reported in Farver's paper. We found a diffusion coefficient for H around thirty to forty times slower along the [010] direction than along [001] and [100]* directions. We should notice that the same type of anisotropy of diffusion was observed by Farver (1989) for oxygen.

The great difference of diffusion rate between H and O in diopside (around ten orders of magnitude) precludes any transport of H through molecular H_2O or OH. Previous work on quartz and olivine have suggested that the diffusivity of H is related to the mobility of interstitial protons (e.g., Kronenberg and Kirby 1986; Mackwell and Kohlstedt 1990). Olivine exhibits also a strong dependence on crystallographic orientation (two orders of magnitude difference between [100] and [010] directions, Mackwell and Kohlstedt 1990).

Mechanism of hydrogen exchange

A charge compensation reaction 1 involving the change of valence of Fe has been proposed for H exchange in mica, amphiboles, olivine and diopside. The change of valence of Fe during dehydroxylation has been confirmed by Mössbauer spec-

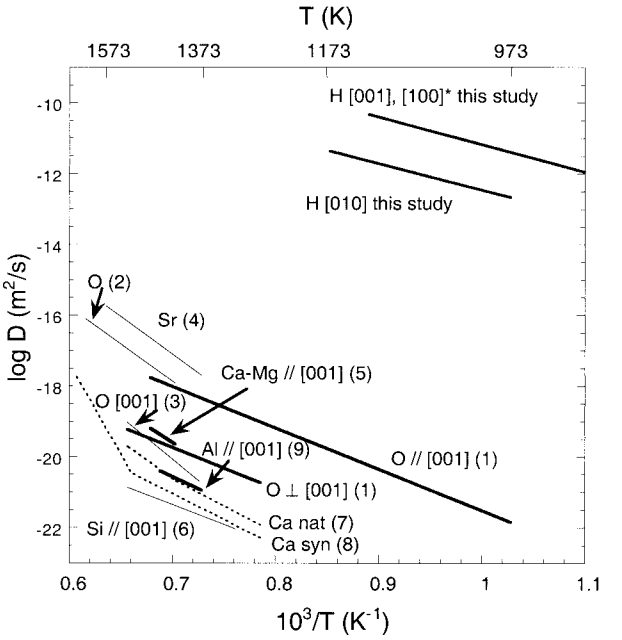

FIGURE 9. Compilation of diffusion laws for various species in diopside. (1) Farver (1989); (2) Connolly and Muehlenbachs (1988); (3) Ryerson and McKeegan (1994); (4) Sneeringer et al. (1984); (5) Brady and McCallister (1983); (6) Béjina and Jaoul (1996); (7) Dimanov et al. (1995); (8) Dimanov and Ingrin (1995); (9) Jaoul et al. (1991).

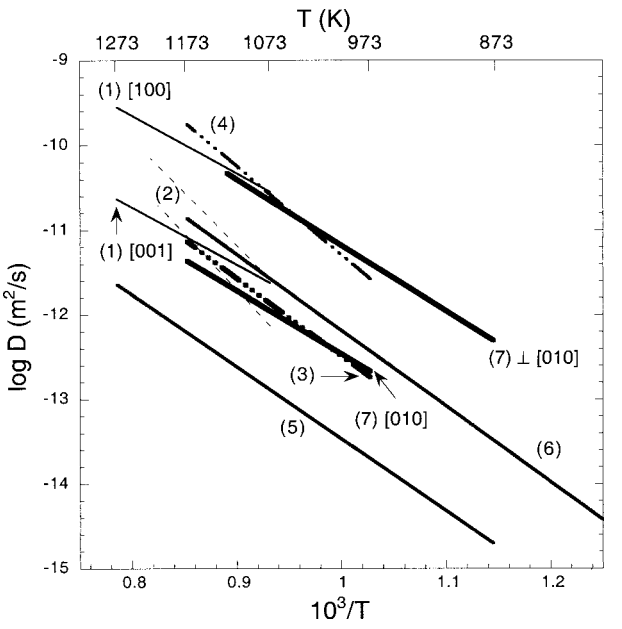

FIGURE 10. Compilation of H diffusion data in different minerals. (1) H in olivine (Mackwell and Kohlstedt 1990); (2) H in pyrope (Wang et al. 1996); (3) H-D in β-quartz (Kats et al. 1962); (4) H in β-quartz (Kronenberg and Kirby 1986); (5) H-D in sanidine and adularia (Behrens 1994); (6) H in adularia (Kronenberg et al. 1996); (7) H-D in diopside (this study).

troscopy performed on amphibole and diopside (Dyar et al. 1992; Skogby and Rossman 1989; Skogby 1994).

Our results show that the H diffusion coefficient measured from H-D exchange is significantly faster than diffusion coefficients measured from H incorporation and extraction experiments (Fig. 7). This indicates that H mobility is not the rate limiting phenomenon of H incorporation or extraction in diopside, as was suggested by earlier deuteration experiments performed by Skogby and Rossman (1989). Mackwell and Kohlstedt (1990) proposed, from H incorporation experiments performed on olivine, that H moves as interstitial protons compensated by a counterflux of electron holes. Thus the kinetic limitation observed in our H incorporation-extraction experiments may come from the lower mobility of electron holes involved in reaction 1. Recent kinetic data, obtained from H extraction experiments performed on diopside single crystals with higher Fe content than the present diopside specimens, lead to faster H exchange closer to the kinetics of H-D experiments (Carpenter 1996; Hercule 1996; Hercule and Ingrin 1996; Carpenter et al. unpublished manuscript). This increase of the kinetics of reaction 1 with Fe content (i.e., with parallel increases in the electron hole concentration) is in accord with the hypothesis of a rate limiting effect of electron hole mobility. Huebner and Voigt (1988) observed also an increase of the diopside conductivity with Fe content suggesting that conduction may be related to a similar mechanism. In our diopside, the mobility of protons would be faster and anisotropic, while the mobility of electron holes would be slower and isotropic. For diopside with higher Fe contents, as the mobility of electron holes becomes faster, the kinetics of H extraction-incorporation (reaction 1) might be expected to increase up to that defined by the mobility of protons. The most recent kinetic data (Carpenter 1996; Hercule 1996; Hercule and Ingrin 1996; Carpenter et al., unpublished manuscript; H. Skogby, personal communication) suggest that above a critical content of about 6 to 8 at% Fe(Fe + Mg), the kinetics of H exchange should be determined by H self-diffusion.

Kinetics of hydrogen exchange in other minerals

In comparison with H diffusion laws for other minerals (Fig. 10), H self-diffusion in diopside occurs very quickly. Kinetic laws for olivine were measured from incorporation experiments (Mackwell and Kohlstedt 1990); the anisotropy of the diffusion as well as the high Fe contain of the olivine samples [Fe/(Fe + Mg) ≈ 9%; San Carlos olivine] suggest that this H exchange is probably controlled by H self diffusion. The same is true for the kinetic laws of H extraction measured by Wang et al. (1996) on pyrope garnets with high Fe content (14 to 20% of almandine component); the diffusion laws obtained can probably be assumed to represent H self-diffusion in garnet. The activation enthalpy found by Mackwell and Kohlstedt for H self-diffusion in olivine is equal to 130 ± 30 kJ/mol, in the same range than our data for H self-diffusion in diopside (around 145 kJ/mol). The activation enthalpy for garnet found by Wang et al. (1996), in the range 240–250 kJ/mol, is much higher than the above enthalpies (but these authors assume a dependence of the kinetic law with H concentration).

For minerals without Fe, like β-quartz (Kats et al. 1962; Kronenberg and Kirby 1986) or feldspars (Behrens 1994; Kronenberg et al. 1996) H-deuteration and uptake experiments have been performed and both experimental conditions lead to activation enthalpies in the range 160–200 kJ/mol.

The comparable activation enthalpies found for H diffusion in diopside and olivine suggests that for these two ferromagnesian minerals diffusion mechanisms are probably the same. By contrast, for non-ferromagnesian minerals like β-quartz and feldspar, but also for garnet (with higher activation enthalpies), H diffusion seems to proceed through a different mechanism.

Hydrogen solubility in diopside

Laboratory measurements at H partial pressure of 0.1 and 1 atm show that the H solubility in diopside following Equation 1 is almost independent of P_{O_2} and temperature in the range 873–1273 K. We know that the present results on H solubility obtained at low temperature are still too preliminary to determine the exact solubility law. The fit of these results to the simple power law given by Equation 8 does not allow a reliable prediction for the H saturation of the crystal at high pH_2. The aim of this determination is to show the potential use of H solubilities in diopside as an independent pH_2 sensor. For instance, the initial value of the integral absorption As of the natural diopside samples used for this study, as they were measured in Ingrin et al. (1995), are close to 160–185 cm^{-2}. Assuming that the power law (Eq. 8) used for the fit of solubility at pH_2 of 0.1 and 1 atm is valid for some range of pH_2 higher than 1 atm, the last pH_2 recorded by the samples in their natural environment can be predicted to be around 2 to 6 atm, values that are compatible with the skarn origin of the samples.

Geological implications

The present results suggest that the kinetics of H exchange in diopside of mantle origin (with higher Fe content than our diopside; see Carpenter et al., unpublished manuscript), is faster than the kinetics deduced from extraction experiments performed by Ingrin et al. (1995). Thus, the conclusions drawn by Ingrin et al. (1995) concerning the lack of direct correlation between H content of mantle xenoliths of the source concentration in H still stands. As these authors mentioned, the H concentration in the nodules probably contains much more information on thermodynamic equilibrium with the magma that carried the nodules, especially with magma chamber conditions prior to eruption, than with the source region. Moreover, the comparable kinetics of H diffusion within diopside and olivine point out that the difference of H contents of natural samples between these two minerals is not relevant to a more rapid loss of H in olivine as was argued earlier (Bai and Kohlstedt 1992, 1993). It is more probably a consequence of the much higher solubility of H in diopside than olivine.

At temperatures up to 1273 K or for short times of heating the H solubility in diopside depends only on H partial pressure. Subject to previous calibrations, IR measurement of H content in clinopyroxenes could thus be used as an independent pH_2 meter. For example, it could be used for volcanic samples that are rapidly quenched by eruption, in low temperature hydrothermal systems or even in piston cylinder experiments.

However, information on H environments in deeper or/and hotter geological conditions (mantle source of xenoliths) could be more difficult to collect. Bai and Kohlstedt (1993) have shown for olivine, at higher temperature, the solubility of H become also dependent on P_{O_2}, as kinetics of formation of intrinsic host defects related to H storage (cation vacancies or oxygen interstitial) become fast enough. Knowledge of the mobility of such defects in diopside is however necessary before determination of the range of temperature or rate of exhumation for which the information would be preserved.

ACKNOWLEDGMENTS

We thank Stephen J. Mackwell and Henrik Skogby for their helpful discussions and communication of their most recent results and Harald Behrens for its fruitful review of the manuscript. M. Steinberg and R. Pichon are acknowledged for providing access to the IR spectrometer and R. Penelle for the access to the 1 atm. hydrogen furnace used for this study. This work was supported by the CNRS-INSU (INSU contribution no. 131, program 97 IT 62).

REFERENCES CITED

Bai, Q. and Kohlstedt, D.L. (1992) Substantial hydrogen solubility in olivine and implications for water storage in the mantle. Nature, 357, 672–674

——(1993) Effects of chemical environment on the solubility and incorporation mechanism for hydrogen in olivine. Physics and Chemistry of Minerals, 19, 460–471.

Behrens, H. (1994) Structural, kinetic and thermodynamic properties of hydrogen in feldpars. In A. Putnis, Ed., Proceedings of a ESF workshop on: Kinetics of cation ordering, p. 1–7. Department of Earth Sciences, University of Cambridge, England.

Béjina, F. and Jaoul, O. (1996) Silicon self-diffusion in quartz and diopside measured by nuclear micro-analysis methods. Physics of the Earth and Planetary Interiors, 97, 145–162.

Bell, D.R. and Rossman, G.R. (1992) Water in earth's mantle: the role of nominally anhydrous minerals. Science, 255, 1391–1397.

Brady, J.B. and McCallister, R.H. (1983) Diffusion data for clinopyroxenes from homogenization and self-diffusion experiments. American Mineralogist, 68, 106–111.

Carpenter, S.J. (1996) The kinetics of hydrogen diffusion in single crystal clinopyroxene, 81 p., Master dissertation, Pennsylvania State University, USA.

Carslaw, H.S. and Jaegger, J.C. (1959) Conduction of heat in solids, 510 p. Clarendon, Oxford, U.K.

Clowe, C.A., Popp, R.K., and Fritz, S.J. (1988) Experimental investigation of the effect of oxygen fugacity on ferric ferrous ratios and unit cell parameters of four natural clinoamphiboles. American Mineralogist, 73, 487–499.

Connolly, C. and Muehlenbachs, K. (1988) Contrasting oxygen diffusion in nepheline, diopside and other silicates and their relevance to isotopic systematics in meteorites. Geochimica Cosmochimica Acta, 52, 1585–1591.

Dimanov, A. and Ingrin, J. (1995) Premelting and high-temperature diffusion of Ca in synthetic diopside: An increase of the cation mobility. Physics and Chemistry of Minerals, 22, 437–442.

Dimanov, A., Jaoul, O., and Sautter, V. (1995) Calcium self-diffusion in natural diopside single crystals. Geochimica Cosmochimica Acta, 60, 4095–4106.

Dyar, M.D., Mackwell, S.J., McGuire, A.V., Cross, L.R., and Robertson, J.D. (1993) Crystal chemistry of Fe^{3+} and H^+ in mantle kaersutite: Implications for mantle metasomatism. American Mineralogist, 78, 968–979.

Dyar, M.D., McGuire, A.V., and Mackwell, S.J. (1992) Fe^{3+}/H^+ and D/H in kaersutites—Misleading indicators of mantle source fugacities. Geology, 20, 565–568.

Farver, J.R. (1989) Oxygen self-diffusion in diopside with application to cooling rate determinations. Earth and Planetary Science Letters, 92, 386–396.

Hercule, S. (1996) Cinétique et solubilité de l'hydrogène dans le diopside monocristallin, 131 p., PhD dissertation, Université Paris-Sud Orsay, France.

Hercule, S. and Ingrin, J. (1996) Hydrogen mobility in diopside. VIth International Symposium on Experimental Mineralogy, Petrology and Geochemistry, Terra abstracts, 8, 28.

Huebner, J.S. and Voigt, D.E. (1988) Electrical conductivity of diopside: Evidence for oxygen vacancies. American Mineralogist, 73, 1235–1254.

Ingrin, J., Hercule, S., and Charton, T. (1995) Hydrogen diffusion in diopside: results of dehydration experiments. Journal of Geophysical Research, 95, 15489–15499.

Ingrin, J., Latrous K., Doukhan J.C., and Doukhan N. (1989) Water in diopside: an electron microscopy and infrared spectroscopy study. European Journal of Mineralogy, 1, 327–341.

Jaoul, O., Sautter, V., and Abel, F. (1991) Nuclear microanalysis: A powerful tool for measuring low atomic diffusivity with mineralogical applications. In J. Ganguly, Ed., Advances in Physical Geochimistry, Diffusion, Atomic Ordering, and Mass Transport: Selected Problems in Geochemistry Vol. 6, p. 198–200. Springer-Verlag, New York.

Kats, A., Haven, Y., and Stevels, J.M. (1962) Hydroxyl groups in ß-quartz. Physics and Chemistry of Glasses, 3, 69–75.

Kronenberg, A.K. and Kirby, S.H. (1986) Solubility and diffusional uptake of hydrogen in quartz at high water pressures: Implications for hydrolitic weakening. Journal of Geophysical Research, 91, 12723–12744.

Kronenberg, A.K., Yund, R.A., and Rossman, G.R. (1996) Stationary and mobile hydrogen defects in potassium feldspar. Geochimica Cosmochimica Acta, 60, 4075–4094.

Le Claire, A.D. (1966) Some comments on the mass effect in diffusion. Philosophical Magazine, 14, 1271–1284.

Mackwell, S.J. and Kohlstedt, D.L. (1990) Diffusion of hydrogen in olivine: implications for water in the mantle. Journal of Geophysical Research, 95, 5079–5088.

Ryerson, F.J. and McKeegan, K.D. (1994) Determination of oxygen self-diffusion in akermanite, anorthite, diopside, and spinel: Implications for oxygen isotopic anomalies and the thermal histories of Ca-Al-rich inclusions. Geochimica Cosmochimica Acta, 58, 3713–3734.

Skogby, H. (1994) OH incorporation in synthetic clinopyroxenes. American Mineralogist, 79, 240–249.

Skogby, H. and Rossman, G.R. (1989) OH in pyroxene: An experimental study of incorporation mechanisms and stability. American Mineralogist, 74, 1059–1069.

Skogby, H., Bell, D.R., and Rossman, G.R. (1990) Hydroxide in pyroxene: Variations in the natural environment. American Mineralogist, 75, 764–774.

Smyth, J.R., Bell, D.R., and Rossman, G.R. (1991) Incorporation of hydroxyl in upper-mantle clinopyroxenes. Nature, 351, 732–735.

Sneeringer, M., Hart, S.R., and Shimizu, N. (1984) Strontium and samarium diffusion in diopside. Geochimica Cosmochimica Acta, 48, 1589–1608.

York, D. (1966) Least-squares fitting of a straight line, Canadian Journal of Physics, 44, 1079–1086.

Wang, L., Zhang, Y., and Essene, E. (1996) Diffusion of the hydrous component in pyrope. American Mineralogist, 81, 706–718.

MANUSCRIPT RECEIVED DECEMBER 21, 1998
MANUSCRIPT ACCEPTED JUNE 6, 1999
PAPER HANDLED BY HANS KEPPLER